Ab Initio Study of the Electronic Excited States in 4-(*N*,*N*-Dimethylamino)benzonitrile with Inclusion of Solvent Effects: The Internal Charge Transfer Process

Benedetta Mennucci,*,† Alessandro Toniolo,‡ and Jacopo Tomasi†

Dipartimento di Chimica e Chimica Industriale, Università di Pisa, via Risorgimento 35, 56126 Pisa, Italy, and Dipartimento di Chimica Fisica ed Elettrochimica, Università di Milano, via Golgi 19, 20133 Milano, Italy

Received March 6, 2000. Revised Manuscript Received August 23, 2000

Abstract: The lower singlet excited states for (dimethylamino)benzonitrile (DMABN) have been studied as a function of the twisting and wagging motion with inclusion of solvent effects. Theoretical calculations have been performed using a multireference perturbed CI method, and the solvent effects have been described within the polarizable continuum model (PCM). In the methodology we have used, solvent interactions are explicitly included in the CI scheme and in the following perturbative corrections, through proper operators corresponding to electrostatic and repulsion interactions. The results obtained including solvent interactions both on geometries and energies support the twisted intramolecular charge transfer (TICT) model proposed to explain the dual fluorescence phenomenon occurring in DMABN when immersed in polar solvents. Calculated transition energies (absorption and emission) obtained for both the isolated and the solvated system are in agreement with available experimental information.

1. Introduction

The interest in the spectroscopic properties of 4-(*N*,*N*-dimethylamino)benzonitrile (DMABN) has attracted increasing attention since the first experimental observations by Lippert et al.[1] The main findings of such experiments were an anormal emission (^1L_a-type according to Platt's notation[2]) in polar solvents, red-shifted from the normal ^1L_b-type fluorescence. This phenomenon, since then known as dual fluorescence, has successively been observed in several other electron donor−acceptor compounds,[3] but DMABN still remains one of the most studied case, and not only for historical reasons. The relatively small dimensions, now easily tractable with standard computational tools, and the numerous experimental data available for comparison have made DMABN a challenging test for different ab initio procedures, and in fact many calculations, of various levels, have been performed, in particular in the past few years. In parallel, and also before these computational efforts, several models have been proposed[1,4,5] to explain the unusual behavior of DMABN and of related compounds. Among all the proposals, that supported by the largest experimental evidence is the twisted intramolecular charge transfer (TICT) model by Grabowski and co-workers.[6]

The TICT model explains the dual fluorescence as occurring by means of a radiationless transition leading to two conformations differing in the dihedral angle between the amino group and the phenyl ring. According to the TICT model the initially promoted excited state yields another minimum on the energy surface by twisting the dialkylamino group from a planar (or nearly planar) to a perpendicular position with respect to the benzonitrile ring. The twisting is accompanied by an intramolecular charge transfer (CT) from the donor (the amino group) to the acceptor moiety (the benzonitrile group) in the excited state. The resulting state (also called CT state), characterized by a large intramolecular charge separation and an increased dipole, can be stabilized by polar solvents, thus leading to the observed "anomalous" ^1L_a-type fluorescence band. The "standard" ^1L_b-type, on the contrary, is assigned to the less polar locally excited (LE) state, where no twisting has occurred.

An alternative explanation to TICT has been proposed by Zachariasse et al.[5] According to the authors, the phenomenon is based on a solvent-induced vibronic coupling between LE and CT states achieved by a sufficiently small energy gap between the two states. In combination with the presence of a promoting mode such as N-inversion of the amino group (usually indicated as wagging motion), this coupling causes a splitting of the quasi-degenerate levels and thereby a consider-

* To whom correspondence should be addressed. Electronic mail: bene@dcci.unipi.it.

† Università di Pisa.

‡ Università di Milano.

(1) Lippert, E.; Lüder, W.; Boos, H. In *Advanced molecular spectroscopy*; Mangini A., Ed.; Pergamon Press: New York, 1962; Vol. 1.

(2) Platt, J. *J. Chem. Phys.* **1949**, *17*, 484.

(3) Rettig, W. *Angew. Chem.* **1986**, *98*, 969; *Angew. Chem., Int. Ed. Engl.* **1986**, *25*, 971; *Top. Curr. Chem.* **1994**, *169*, 253.

(4) Khalil, O. S.; Hofeldt, R. H.; McGlynn, S. P. *Chem. Phys. Lett.* **1972**, *17*, 479. (b) Kosower, E. M.; Dodiuk, H. *J. Am. Chem. Soc.* **1976**, *98*, 924. (c) Chandross, E. A. In *Exciplex*; Gordon, M., Ware, W. R., Eds.; Academic Press: New York, 1975. (d) Visser, R. J.; Weisenborn, P. C. M.; Varna, C. A. G. O. *Chem. Phys. Lett.* **1985**, *133*, 330.

(5) Schuddeboom, W.; Jonker, S. A.; Warman, J. M.; Leinhos, U.; Kühnle, W.; Zachariasse, K. A. *J. Phys. Chem.* **1992**, *96*, 10809. (b) Zachariasse, K. A.; von der Haar, T.; Leinhos, U.; Kühnle, W.; J. *Inf. Rec. Mater.* **1994**, *21*, 501. (c) Leinhos, U.; Kühnle, W.; Zachariasse, K. A. *J. Phys. Chem.* **1991**, *95*, 2013. (d) Zachariasse, K. A.; von der Haar, T.; Hebecker, A.; Leinhos, U.; Kühnle, W. *Pure Appl. Chem.* **1993**, *65*, 1745. (e) Zachariasse, K. A.; Grobys, M.; von der Haar, T.; Hebecker, A.; Il′ichev, Y.; Morawski, O.; Rückert, I.; Kühnle, W. J. *Photochem. Photobiol. A: Chem.* **1997**, 105, 373. (f) Zachariasse, Z. A. *Chem. Phys. Lett.* **2000**, *320*, 8.

(6) Rotkiewicz, K.; Grellmann, K. H.; Grabowski, Z. R. *Chem. Phys. Lett.* **1973**, *19*, 315. (b) Grabowski Z. R.; Rotkiewicz, K.; Siemarczuk, A.; Cowley, D. J.; Baumann, W. *Nouv. J. Chim.* **1979**, *3*, 443.

10.1021/ja000814f CCC: $19.00
Published on Web 10/18/2000

able energetic stabilization of one state. This represents the charge transfer state leading to the second fluorescence band. In this connection, the term pseudo Jahn−Teller coupling has been introduced even if the authors use the PICT acronym where P stands for planar.

Numerous theoretical studies on DMABN using both semiempirical and ab initio methods have been carried out,[7−10] and many of them confirm the greater validity of the TICT model with respect to the Jahn−Teller alternative. The main body of such calculations, however, has been limited to the isolated system, while few examples including solvent effects can be quoted.[11−14] On the contrary, the phenomenon is strongly related to solvation and thus explicit considerations of solvent interactions are very important to obtain a more accurate understanding of the experimental evidence.

In the following sections we present an attempt in this direction, reporting a correlated study of DMABN both in vacuo and in solution. In particular, we use the multireference perturbation configuration interaction (CI) method, known by the CIPSI acronym,[15] which very recently[16] has been coupled to the solvation continuum model originally developed in Pisa in 1981[17] but almost completely revised in the last 2 years. The revised version is more commonly indicated as PCM-IEF (polarizable continuum model within a new integral equation formalism).[18]

As the CIPSI method is not supported by analytical derivatives, all the geometry optimizations both in vacuo and in solution have been obtained with other methods: the density functional (DFT) procedure for ground states and the configuration interaction method including only single excitations (more often indicated as CI-singles, CIS, or Tamm Dancoff approximation, TDA) for excited states. The extension of PCM-IEF to analytical gradients,[19] either at the Hartree−Fock or DFT level, has already been applied to many different systems; on the contrary, CIS analytical derivatives for PCM-IEF solvated systems is a very recent implementation which has been tested just on the excited states of DMABN;[20] in the following we shall exploit the geometries presented in the reference paper.[20]

Because of the many features involved in the analysis, we chose to partition the results in three subsections; first we performed a detailed analysis of the potential energy surfaces (PES) of the ground and the lowest singlet excited states in the gas phase, considering both the twisting and the wagging motions of the dialkylamine group. Then we focused the attention on a more limited section of these surfaces, namely, that concerning the twisting mode only, and we included explicit solvent effects; we chose acetonitrile as an example of a polar solvent. Finally, we further restricted the analysis to transition (absorption and fluorescence) energies in vacuo and in solution; for the fluorescing excited states we used CIS optimized geometries, and for both absorbing and emitting vertical processes, we introduced nonequilibrium conditions between solute and solvent. As a comparison we calculated absorption and fluorescence energies for a second, apolar, solvent (cyclohexane).

2. Methods and Computational Details

The labeling of the atoms of DMABN we shall adopt in the following is reported below:

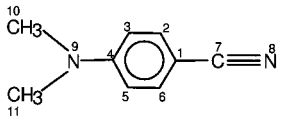

Ground state (GS) geometry optimizations both in vacuo and in solution have been obtained at DFT level employing the nonlocal exchange correlation functional of Becke and Lee, Yang, and Parr in its hybrid form, i.e., including some portion of exact HF exchange (B3LYP),[21] while gas-phase and solvated excited states have been optimized at CIS level; in all cases a 6-31G(d) basis set has been used.

Both DFT and CIS calculations (either for the isolated and the solvated systems) have been performed by exploiting a development version of the Gaussian code.[22] The details on the implementation of PCM-IEF into the CIS algorithm can be found in ref 20, as well as all the comments on solvent effects on the geometries of both ground and excited states.

All the results we shall present below have been obtained through the CIPSI method. These calculations have been carried out by interfacing the original algorithm, modified as described in ref 16 to take into account the solvent, to a development version of the GAMESS package[23] in which the PCM-IEF model has been implemented. See ref 16 for technical details on this interface. In the CIPSI calculations we have excluded the d basis functions for both carbons of the amino group in order to obtain a more manageable basis set (we recall that we do not freeze any virtual orbital, i.e., every molecular orbital should be correlated). At each molecular geometry, both in solvent and in vacuo, the "aimed selection" [24] is run in order to define a variational

(7) Serrano-Andrés, L.; Merchan, M.; Roos, B. O.; Lindh, R. *J. Am. Chem. Soc.* **1995**, *117*, 3189.

(8) Sobolewski, A. L.; Domcke, W. *Chem. Phys. Lett.* **1996**, *250*, 428. (b) Sobolewski, A. L.; Domcke, W. *Chem. Phys. Lett.* **1996**, *259*, 119. (c) Sobolewski, A. L.; Sudholt, W.; Domcke, W. *J. Phys. Chem. A* **1998**, *102*, 2716. (d) Sudholt, W.; Sobolewski, A. L.; Domcke, W. *Chem. Phys.* **1999**, *240*, 9.

(9) Parusel, A. B. J.; Kohler, K.; Grimme, S. *J. Phys. Chem. A* **1998**, *102*, 6297.

(10) Parusel, A. B. J.; Kohler, K.; Nooijen, M. *J. Phys. Chem. A* **1999**, *103*, 4056.

(11) Broo, A.; Zerner, M. C. *Chem. Phys. Lett.* **1994**, *227*, 551.

(12) Scholes, G. D.; Phillips, D.; Gould, I. R. *Chem. Phys. Lett.* **1997**, *266*, 521. (b) Scholes, G. D.; Gould, I. R.; Parker, A. W.; Phillips, D. *Chem. Phys.* **1998**, *234*, 21.

(13) Gedeck, P.; Schneider, S. J. *Photochem. Photobiol. A: Chem.* **1997**, *105*, 165; (b) **1999**, *121*, 7.

(14) Dreyer, J.; Kummrow, A. *J. Am. Chem. Soc.* **2000**, *122*, 2577.

(15) Huron, B.; Malrieu, J.-P.; Rancurel, P. *J. Chem. Phys.* **1973**, *58*, 5745. (b) Evangelisti, S.; Daudey, J.; Malrieu, J.-P. *Chem. Phys.* **1983**, *75*, 91. (c) Spiegelmann, F.; Malrieu, J.-P. *J. Phys. B* **1984**, *17*, 1235. (d) Cimiraglia, R. *J. Chem. Phys.* **1986**, *83*, 1746. (e) Cimiraglia, R.; Persico, M. *J. Comput. Chem.* **1987**, *8*, 39.

(16) Mennucci, B.; Toniolo, A.; Cappelli, C. *J. Chem. Phys.* **1999**, *110*, 6858.

(17) Miertus, S.; Scrocco, E.; Tomasi, *J. Chem. Phys.* **1981**, *55*, 117. (b) Cammi R.; Tomasi, J. *J. Comput. Chem.* **1995**, *16*, 1449.

(18) Cancès, E.; Mennucci, B. J. Math. Chem. **1998**, *23*, 309. (b) Cancès, E.; Mennucci, B.; Tomasi, J. *J. Chem. Phys.* **1997**, *107*, 3032. (c) Mennucci, B.; Cancès, E.; Tomasi, J. *J. Phys. Chem. B* **1997**, *101*, 10506.

(19) Cancès, E.; Mennucci, B. *J. Chem. Phys.* **1998**, *109*, 249. (b) Cancès, E.; Mennucci, B.; Tomasi, J. *J. Chem. Phys.* **1998**, *109*, 260.

(20) Cammi, R.; Mennucci, B.; Tomasi, J. *J. Phys. Chem. A*, **2000**, *104*, 5631.

(21) Becke, A. *J. Chem. Phys.* **1993**, *98*, 5648. (b) Stephens, P. J.; Devlin, F. J.; Chabalowski, C. F.; Frisch, M. J. *J. Phys. Chem.* **1994**, *98*, 11623.

(22) Frisch, M. J.; Trucks, G.W.; Schlegel, H. B.; Scuseria, G. E.; Robb, M. A.; Cheeseman, J. R.; Zakrzewski, V. G.; Montgomery Jr, J. A.; Stratmann, R. E.; Burant, J. C.; Dapprich, S.; Millam, J. M.; Daniels, A. D.; Kudin, K. N.; Strain, M. C.; Farkas, O.; Tomasi, J.; Barone, V.; Cossi, M.; Cammi, R.; Mennucci, B.; Pomelli, C.; Adamo, C.; Clifford, C. S.; Ochterski, J.; Petersson, G. A.; Ayala, P. Y.; Cui, Q.; Morokuma, K.; Malick, D. K.; Rabuck, A. D.; Raghavachari, K.; Foresman, J. B.; Cioslowski, J.; Ortiz, J. V.; Stefanov, B. B.; Liu, G.; Liashenko, C. A.; Piskorz, P.; Komaromi, I.; Gomperts, R.; Martin, R. L.; Fox, D. J.; Keith, T.; Al-Laham, M. A.; Peng, C. Y.; Nanayakkara, A.; Gonzalez, C.; Challacombe, M.; Gill, P. M. W.; Johnson, B.; Chen, W.; Wong, M. W.; Andres, J .; Head-Gordon, M.; Replogle, E. S.; Pople J. A. *Gaussian 99, Development Version*; Pittsburgh, 1999.

(23) Schmidt, M.W.; Baldridge, K. K.; Boatz, J. A.; Elbert, S. T.; Gordon, M. S.; Jensen, J. H.; Koseki, S.; Matsunaga, N.; Nguyen, K. A.; Su, S. J.; Windus, T. L.; Dupuis, M.; Montgomery, J. A. *J. Comput. Chem.* **1993**, *14*, 1347.

(24) Angeli, C.; Persico, M. *Theor. Chem. Acc.* **1997**, *98*, 117.

subspace of electronic configurations, giving a balanced description of all the electronic states of interest: three singlet states for solvent calculations and five singlet states for calculations in vacuo.

The calculations in vacuo are made in a single CIPSI macroiteration constituted by three perturbative selections (microiterations). For the calculations in solution, we repeat CIPSI macroiterations until convergency of the final variational energy for each electronic state (see below). The variational wave functions, expanded over up to about 10000 selected determinants, are the basis for a diagrammatic quasi-degenerate perturbation theory treatment,[15,25] with a Møller−Plesset (MP) partition of the Hamiltonian.

As important features of the solvation model we recall that in the PCM-IEF[18] the solute charge distribution is assumed to occupy a volume of known shape and dimension (i.e., the molecular cavity), while the solvent, treated as an infinite continuum dielectric, is represented in terms of specific operators (usually indicated with the comprehensive term V^R) defined on the cavity surface. The latter are added to the Hamiltonian of the isolated system (H^0) to obtain the final effective Hamiltonian and the related Schrödinger equation in a form completely equivalent to that defined in vacuo. The main difference is that now the solvent terms, in part depending on the solute wave function they contribute to modify, give origin to an additional nonlinearity. In this case the variational solution of the Schrödinger equation is obtained by minimizing a new functional which presents the status of a free energy; namely, we have

$$G(\Psi) = \langle\Psi|H^0|\Psi\rangle + \langle\Psi|{V_p}^R|\Psi\rangle + \frac{1}{2}\langle\Psi|{V_{wf}}^R|\Psi\rangle \qquad (1)$$

where we have introduced an explicit partition of the solvent terms into their constant (${V_p}^R$) and wave function dependent (${V_{wf}}^R$) contributions, respectively. The detailed description of the various terms appearing in eq 1 can be found in the already quoted ref 18 and in the references therein.

The definition of the free energy functional (1) and of the related solvent operators, ${V_p}^R$ and ${V_{wf}}^R$, is the basic aspect common to all the levels of calculation (DFT, CIS and CIPSI) exploited in the present paper; differences appear as soon as we enter more deeply into the specific features of each method. The interested reader is referred to the original papers on the various extensions of PCM-IEF, namely ref 26 for a brief review on various applications to HF and DFT theory, ref 20 for CIS, and ref 16 for CIPSI. Here, we only recall some further details on CIPSI calculations.

As said before, gas-phase calculations are made by a single macroiteration (see ref 16 for the terminology) constituted by three perturbative selections (microiterations); on the contrary, in the presence of the solvent CIPSI macroiterations are repeated until convergency of the final variational energy for each electronic state. We need this self-consistent scheme because of the nonlinear dependence of the solvent reaction potential on the solute wave function.

We also recall that in the current PCM-IEF version the solvent perturbative operators account for both electrostatic and repulsive effects; in particular, to describe repulsion interactions between solute and solvent we have used the model originally formulated by Amovilli and Mennucci.[27] In brief, we also note that two different solvation models have been used, namely, assuming equilibrium or nonequilibrium conditions between solute and solvent charge densities, respectively. In the former case, a fully equilibrated system is assumed while in the latter case (coinciding with transition phenomena) delays in the solvent response with respect to the solute electronic changes are considered. Detailed descriptions of formal and numerical aspects of these two different approaches will be given in the following.

The properties to be defined in a PCM-IEF calculation are some cavity parameters and the solvent dielectric constant. Here, the solute is embedded in a molecular cavity obtained in terms of interlocking spheres centered on the heavy nuclei (6 C of the benzene ring, C and N of nitrile and N, and 2 C of dimethylamino group). The chosen radii are 1.9 for the four hydrogen-bonded aromatic carbons and 1.7 for both the other two carbon atoms of the ring and for the nitrile carbon, 2.0 for the two methyl carbons, and 1.6 for both the nitrile and the amino N. All the radii have then been multiplied by 1.2 to take into account the impenetrating core of the solvent molecules.[28] Finally, values of 36.64 and 2.02 for the static dielectric constants and of 1.806 and 2.02 for the optical analogues have been used to represent acetonitrile and cyclohexane solvents, respectively; the roles of these pairs of values will be explained in more detail in the last subsection devoted to absorption and fluorescence energies.

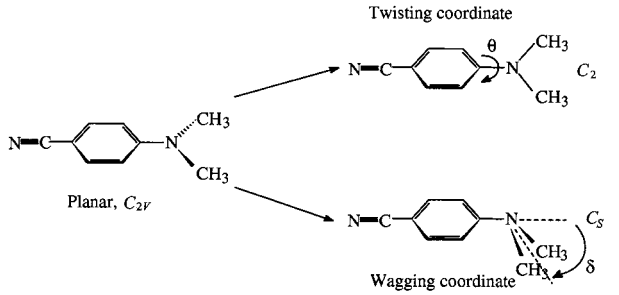

Figure 1. Schematic representation of the DMABN twisting and wagging coordinates.

3 Results

3.1. Potential Energy Surfaces (PES) in the Gas Phase. We studied the CIPSI potential energy surfaces of the first five singlet states of the DMABN along two coordinates starting from the geometry of the ground state (GS). We note that the B3LYP/6-31G(d) optimized geometry of the GS is found to be planar, possessing C_{2v} symmetry. On the contrary, experiments seem to confirm a slight pyramidalization angle of the amino group of the order of 12−15°.[29] Previous calculations[9] still exploiting DFT methods have shown that such a nonplanar structure can be obtained using larger basis sets, but the same calculations also show that the effects of this small pyramidalization angle are insignificant for a discussion of the photophysical behavior of DMABN. Supported by these studies, in the present paper we have not extended the calculation to larger basis sets, and our analyses have thus been based on a planar GS both in vacuo and in solution.

Starting from such planar structure, we independently move the two dihedral angles (D_1 and D_2) defined by the two carbon atoms of the amino group and the aromatic ring; namely, $D_1 = \tau(C_{10}N_9C_4C_3)$ and $D_2 = \tau(C_{11}N_9C_4C_5)$. We then define the twisting angle θ as $^1/_2(D_1 + D_2)$ and the wagging angle δ as $^1/_2(D_1 + D_2)$. By changing both dihedral angles of the same amount and with the same sign, we can explore the pure twisting coordinate of the amino group (along the bond between the amino nitrogen and the aromatic carbon). Along this coordinate which represents the leading parameter of the TICT model, a C_2 symmetry is maintained. Because of this symmetry constraint, the electronic states can be classified as A or B singlets (these will be the labels used in the next section concerning energy profiles along the single twisting coordinate). On the contrary, when we change both angles by the same amount but with opposite sign, we obtain the wagging coordinate of the amino group; in this case the maintained symmetry is C_s (if the twisting angle is 0° or 90°). Here the states can be labeled as A′ and A″. The two angles are represented in Figure 1.

(25) Angeli, C.; Cimiraglia, R.; Persico, M.; Toniolo, A. *Theor. Chem. Acc.* **1997**, *98*, 57.
(26) Tomasi, J.; Mennucci, B.; Cancès, E. *J. Mol. Struct.: THEOCHEM* **1999**, *211*, 464.
(27) Amovilli, C.; Mennucci, B. *J. Phys. Chem. B* **1997**, *101*, 1051.
(28) Tomasi, J.; Persico, M. *Chem. Rev.* **1994**, *94*, 2027.
(29) Heine, A.; Herbst-Irmer, R.; Stalke, D.; Kühnle, W.; Zachariasse, K.A. *Acta Crystallogr.* **1994**, *B50*, 363. (b) Kajimoto, O.; Yokoyama, H.; Ooshima, Y.; Endo, Y. *Chem. Phys. Lett.* **1991**, *179*, 455.

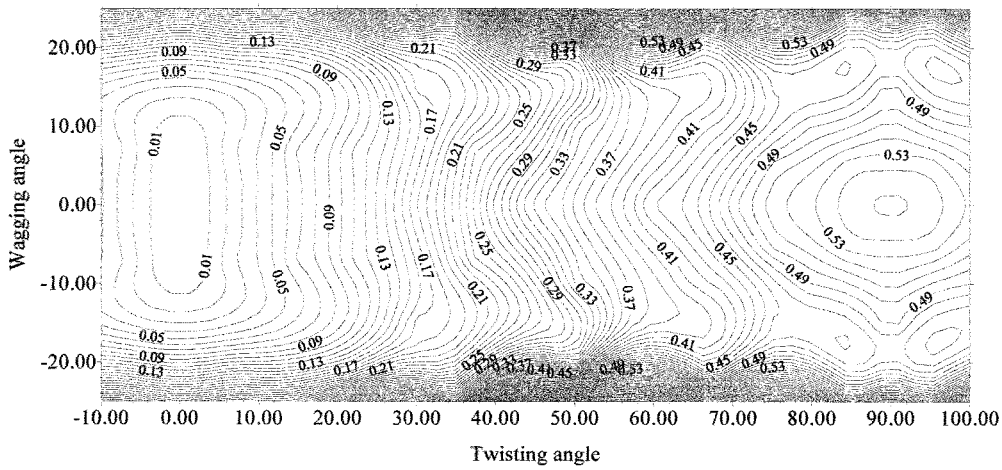

Figure 2. Planar projection of the twisting−wagging energy surface for the ground state of DMABN. Energy levels (in eV) are computed with respect to the value corresponding to 0° wagging and 0° twisting.

Finally, when we explore the whole surfaces scanned by the two angles, no symmetry is maintained. Therefore, in the following surfaces we shall adopt the conventional classification: S_0 for the ground state and S_1, S_2 ... for the excited states in order of energy.

In Figures 2-4 we report the planar projection with respect to the wagging and twisting angles of the energy surfaces obtained as interpolation of 147 points from 48 different CIPSI calculations. For the two lowest excited state S_1 and S_2, we also report the corresponding 3D maps.

As shown in Figure 2 the ground state (S_0) presents a valley along the twisting coordinate. The minimum is located at the full planar geometry. We adopt the energy of this minimum as energy reference. For small displacements, the twisting induces higher energy increments with respect to the wagging, as it gives rise to a decrease in the overlap between the lone pair p orbital of the amino nitrogen (lpN) and the π aromatic orbitals. On the contrary, for larger displacements, the wagging coordinate produces a rapid increase in the potential energy because of the repulsion of the two methyl groups. The pure twisting coordinate presents a maximum at 90°; the energetic barrier is 0.55 eV. However, we found a transition state at 0.47 eV for a wagging angle of 17.5°; it is in fact the nonzero wagging that allows the twisting along the bond between the aminic nitrogen and the aromatic ring to follow a lower energy channel.

The first excited state S_1 (see Figure 3) shows a more complex structure: here the minimum of the energy (4.20 eV) is found at the same geometry of the S_0 ($\theta = 0°$ and $\delta = 0°$), even if there appear two further flat regions at 4.26 eV centered at a twisting angle of 20° and a wagging angle of 12° and −12°. Going along the twisting coordinate we found a cusp at 4.50 eV near 45°; this is the conical intersection between S_1 and the following S_2 state. Beyond this point there is another well: the minimum is located around 80° along the pure twisting coordinate at about 4.28 eV. We note that along the twisting coordinate ($\delta = 0°$) this state has B symmetry from $\theta = 0°$ to the conical intersection and symmetry A after.

The S_2 state (see Figure 4) presents a large flat region around the planar conformation until $\theta = 0°$ (at about 4.80 eV), when it decreases toward the conical intersection at 4.50 eV. Then the energy increases until $\delta = 90°$. As previously reported for state S_1, for S_2 we note that along the twisting coordinate its symmetry changes from A (from $\theta = 0°$ to the conical intersection) and B after that.

Further details on the electronic nature and the properties of the two states will be given in the next section.

The energy maps of the following two states are not reported as these states are not really involved in the photochemistry of DMABN; we only recall that S_3 shows a minimum region at 5.40 eV centered around $\theta = 90°$ and an higher zone near the planar configuration at about 6.20 eV, whereas S_4 presents high energies at small twisting angles which continuously decrease toward an almost planar region (around 6.40 eV) going from $\theta = 30°$ to $\theta = 90°$.

3.1.1. Analysis of Wagging and Twisting Modes. The energy maps above permit us to analyze, and compare, the relative importance of the two motions, represented by the wagging and twisting coordinates, with respect to possible channels leading to the charge transfer process. In particular, the main result we can extract from Figures 2−4 is that the wagging motion cannot be the only mechanism promoting the charge-transfer process. In fact, on the one hand, the energy of each state increases so much along the δ coordinate to exclude a large motion along this coordinate, while the twisting coordinate represents a reliable channel which involves small energy variations. On the other hand, and even more important, the first excited-state surface does not present a pseudo Jahn−Teller effect such as that introduced by Zachariasse et al.;[5] concerning this point some further comments are required.

We recall that in Zachariasse model (also indicated as PICT),[5] when the two excited states are sufficiently close in energy, a change in the amino group (from pyramidal to planar) allows a vibronic coupling between them with formation of a charge transfer state. Besides this basic structural change the global process will involve also changes of the bond lengths in the molecule. Such further structural effects are not taken into account in our analyis; however, we can still try to extract some information on the validity of this hypothesis from our results. From Figures 3 and 4 we see that the only chance for such a mechanism is at the position of the conical intersection. If we consider the section along the wagging coordinate passing through this point, a characteristic double minima of the state is indeed observed but with a shallow depth of only 0.06 eV.

These results actually do not add too much to the real understanding of the phenomenon under scrutiny as limited to the gas-phase in which the CT-induced dual fluorescence is not observed; it is thus interesting to see if such a process happens in solution. To obtain a numerical confirmation, we performed CIPSI calculations for the two lowest excited states in an acetonitrile solution. The interesting section of the surface is in this case centered on the planar structure; it is in fact that

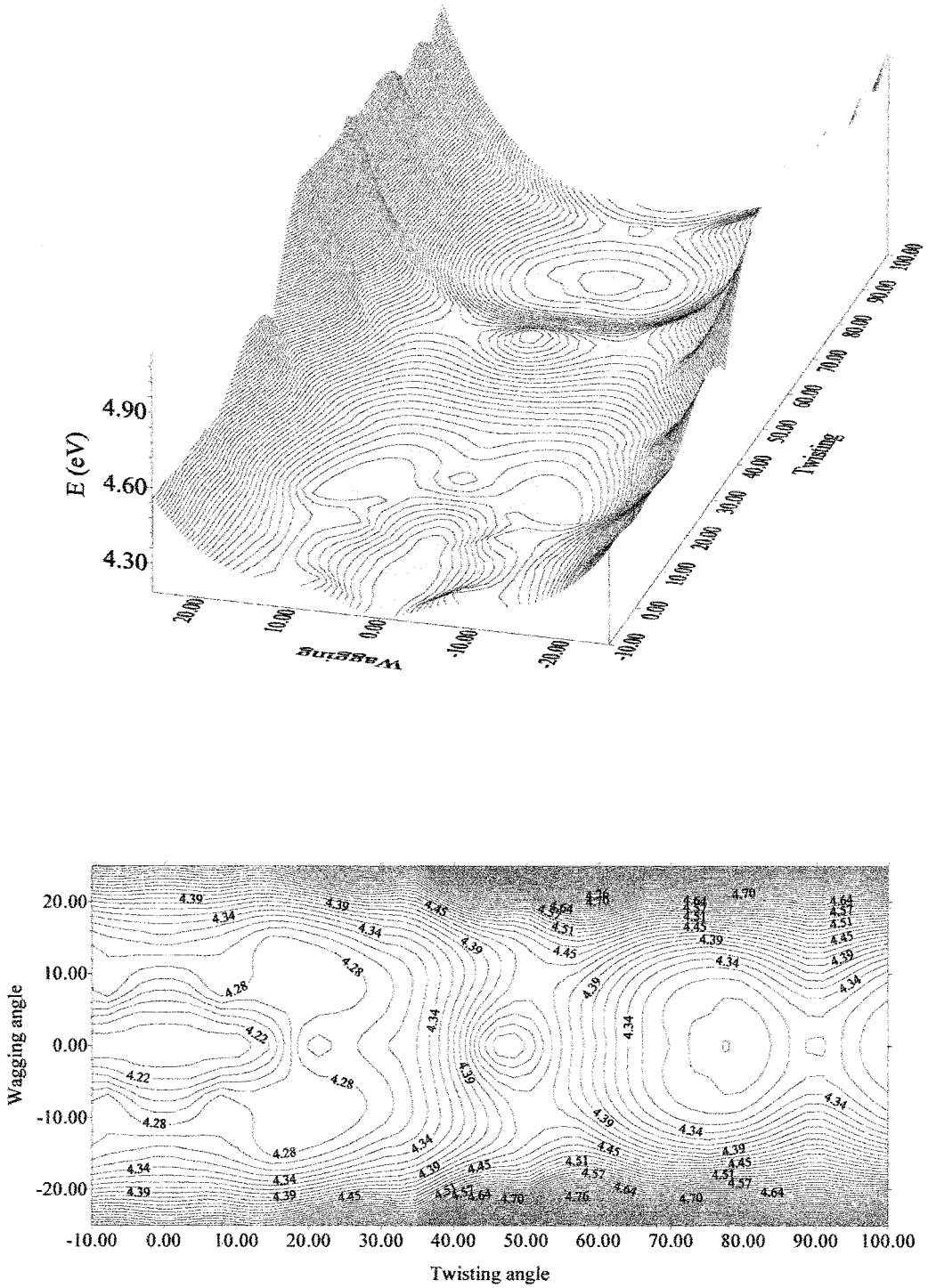

Figure 3. Twisting−wagging energy surface and its planar projection for the first singlet excited state (S_1) of DMABN. Energy values (in eV) are computed with respect to ground-state minimum (0° wagging and 0° twisting).

invoked by Zachariasse as the final equilibrated charge-transfer structure. Following this suggestion, we changed the wagging angle from −20°/+20° with a step of 5° and maintained all the other geometrical parameters at the values optimized for the solvated ground state (and hence without any twisting of the amino group). We note that in solution the order of the two excited states found for the isolated system is reversed; already at 0° twisting the lowest state is the A state; a detailed analysis of this result will be reported in the next section.

The results we have obtained show that the two excited states, even if very close in energy at the planar structure as required by the Zachariasse model, do not present any important variation along the wagging coordinate either in the energy or in the dipole. In particular, the energy difference between the minima of the two states is less than 0.01 eV and the dipole of the more polar state slightly decreases from the planar largest value thus showing no significant change in the charge distribution along this coordinate. The combination of these results seems to suggest that the wagging motion alone is unable to produce the charge transfer expected for the lower energy fluorescence in polar solvents.

All these evidences, even if affected by the effects of the frozen-geometry approximation we have adopted, have led us to exclusively focus on the alternative TICT model and not

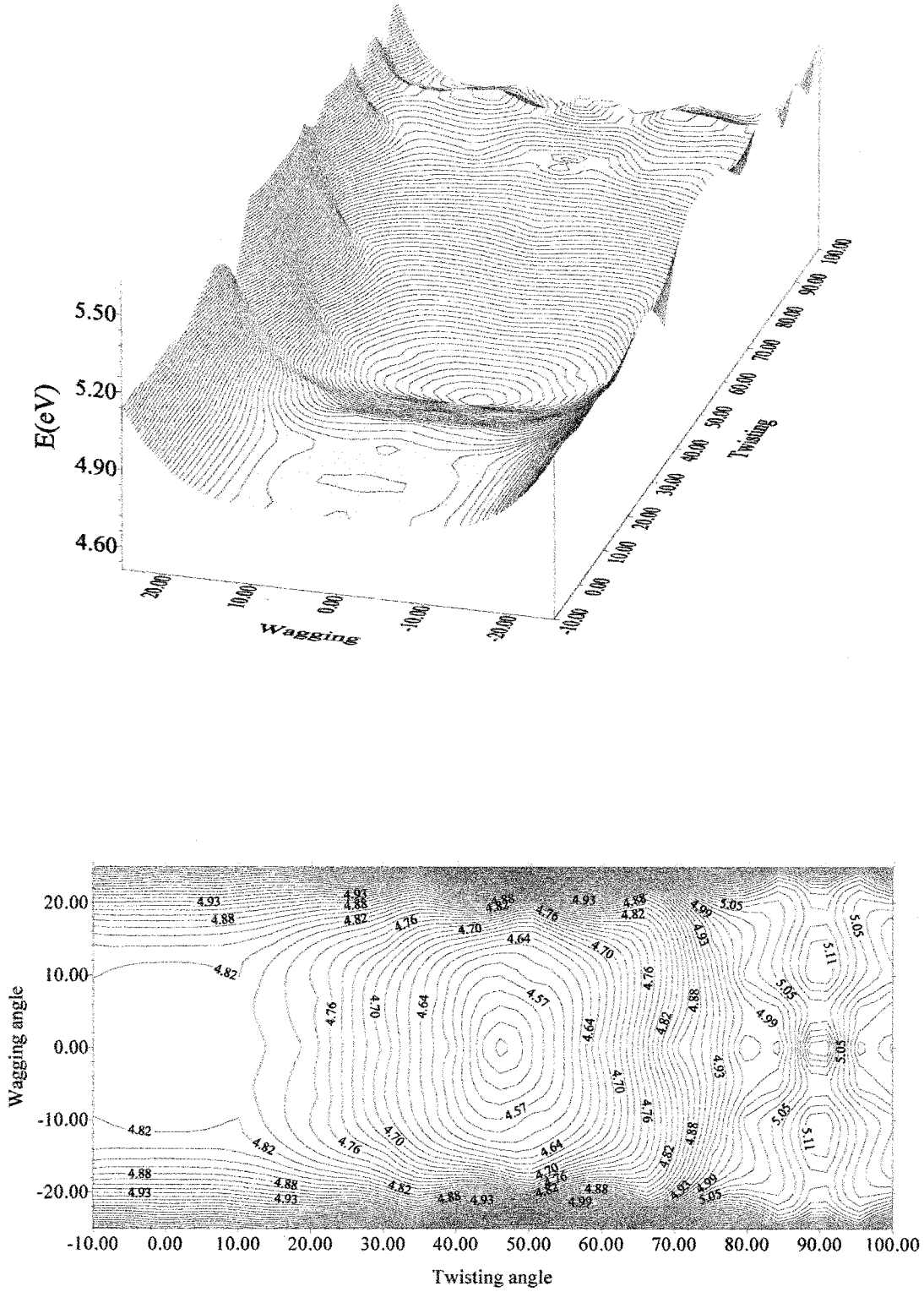

Figure 4. Twisting−wagging energy surface and its planar projection for the second singlet excited state (S_2) of DMABN. Energy values (in eV) are computed with respect to ground-state minimum (0° wagging and 0° twisting).

pursue the analysis of the wagging motion (and the related Jahn−Teller hypothesis) any further.

3.2. Twisting Curves in Vacuo and in Acetonitrile Solution. As in the evaluation of the energy maps presented in the previous subsection, for the following curves the geometry has been kept frozen to that optimized for the ground state (i.e., with a wagging angle equal to zero) at any point and for any electronic state; the only changing parameter is the twisting angle θ which has been varied from 0° to 90° in steps of 15°. All the points have been calculated at the CIPSI level both in vacuo and in acetonitrile solution, preserving a C_2 symmetry. In addition, for calculations in solution, an equilibrium description has been used; here, in fact, the interest is not focused on transition phenomena, which could imply delays in the solvent response with respect to solute electronic changes but on the analysis of sections of PES. In this case we can assume that solute and solvent can always completely equilibrate. Consideration of possible delays, and, as a consequence, of nonequi-

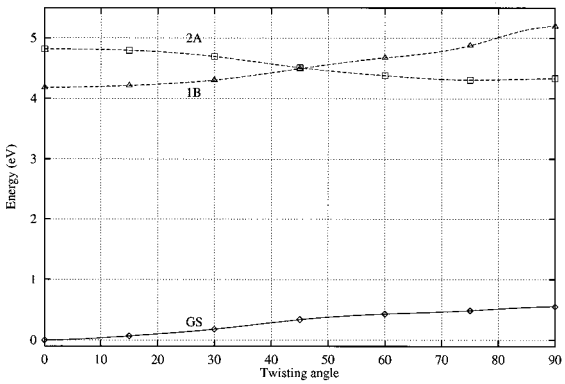

Figure 5. Ground and low-lying singlet excited states potential curves (energy relative to the minimum of the ground state) of DMABN in vacuo as a function of the twisting angle. Energies are in eV and angles in degrees.

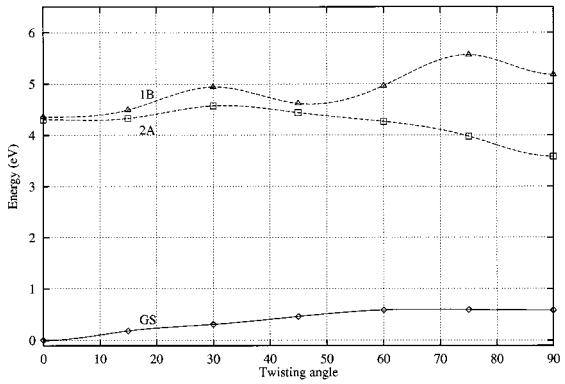

Figure 6. Ground and low-lying singlet excited states potential curves (energy relative to the minimum of the ground state) of DMABN in acetonitrile as a function of the twisting angle. Energies are in eV and angles in degrees.

libria between solute and solvent will become compulsory in the analysis of absorption and/or fluorescence energies reported in the next section.

The results for the ground and the two lowest excited states of both isolated and solvated DMABN are presented in Figures 5 and 6, respectively. All energies are relative to those of the corresponding ground state at the nontwisted geometry ($\theta = 0°$).

Inspection of the potential curves along the twisting path, as expected, shows very different features for isolated and solvated systems.

As reported in previous calculations,[7,9,10] gas-phase results are characterized by the two lowest singlet excited states which cross at a twisting angle near 45°. In particular, the most stable excited state at the nontwisted geometry presents a maximum at perpendicular geometry, while the second one shows a completely reversed behavior, thus inducing the crossing of the corresponding curves. The two states for which 1^1B and 2^1A labels are used according to the C_2 symmetry can be identified with the L_b-type, or LE, state and the L_a-type, or CT, state, respectively. The observed crossing is here allowed due to the differences in the intrinsic symmetry character of the two states. An analysis of the CIPSI wave function shows that the first excited state (1^1B) at nontwisted conformation is dominated by the HOMO $\rightarrow$ LUMO + 1 and HOMO − 1 $\rightarrow$ LUMO single excitations, where the involved orbitals are benzene ring π (for the two occupied) and π^* (for the two unoccupied) orbitals.

Also the other state (2^1A) is dominated by a single excited configuration. At the nontwisted geometry the wave function is mainly composed of the HOMO $\rightarrow$ LUMO excitation; it should be noted that the HOMO orbital includes a strong mixing with the N amino lone pair orbital (lpN). It is the excitation from this orbital (i.e., the transition lpN $\rightarrow$ LUMO or better n $\rightarrow \pi^*$) that becomes the most important at the twisted conformation. At this conformation the lone pair orbital is no more mixed with the π system and, as a consequence, it is destabilized up to the HOMO level. The partial lpN character of the HOMO orbital observed in the nontwisted wave function of the 2^1A state shows that some of the charge transfer inferred by the n $\rightarrow \pi^*$ transition is already included. As we shall show, this mixing acquires an important role in the presence of a polar solvent.

In the presence of a polar solvent the same curves become significantly different as the highly polar 2^1A state can be stabilized much more effectively than the less polar 1^1B state, thus inverting their relative energies even at a nontwisted geometry. To the best of our knowledge this behavior was found only once before, in the calculations by Gedeck and Schneider;[13] all other previous studies including solvent effects in fact showed the preferential stabilization of the A state with respect to B but only limited to a few specific conformations and not along the energy profiles.

Some further comments can be derived from the orbital analysis. The 2^1A state is mainly dominated by the singly excited configuration HOMO $\rightarrow$ LUMO exactly as in vacuo; here, however, the partial mixing among the benzene π orbitals and N lone pair we have already found for the HOMO orbital in the isolated system is largely increased as well as the percent of charge-transfer character of the state. Qualitatively this means that the solvent can interact more effectively with this state, lowering its energy below the other one involving only n $\rightarrow \pi^*$ excitations.

The second important characteristic of Figure 6 is the large stabilization of the 2^1A state at the twisted geometry which represents the global minimum in the curve; the twisted conformation lies ~19.5 kcal/mol below the planar one, and the thermodynamic equilibrium of the charge-transfer reaction is therefore almost totally shifted to the twisted conformation. This result seems to support the interpretation of the dual fluorescence in terms of the TICT model. It is worth noting that this large stabilization and not the relative values of the barrier between nontwisted and twisted geometries could represent the most significant feature. In fact, these curves do not represent the lowest energy path on the multidimensional energy surface and thus the barrier we can estimate from them is a very rough approximation. Anyway, assuming that the definition of such barrier as the energy difference between the minimum of the B state and the energy maximum in the path going to the A minimum is valid, the computed results show a significant decrease in the barrier height (from 7 to 5 kcal/mol from vacuo to solution), in qualitative agreement with experiments (see ref 13 and references therein).

A parallel analysis can be obtained in terms of change in the dipole moment values for the different electronic states with respect to the twisting coordinate. Such an analysis is reported in Figures 7 and 8 for the three previous singlet states (GS + two lowest excited states) both in vacuo and in acetonitrile.

The ground-state dipole moments for the isolated and the solvated systems are very similar in their general trend. They decrease with increasing twisting angle; the only difference is in the absolute values, which are always greater in solution. The dipole moment of the 1^1B state decreases in going from the planar to the twisted structure in both gas phase and solution.

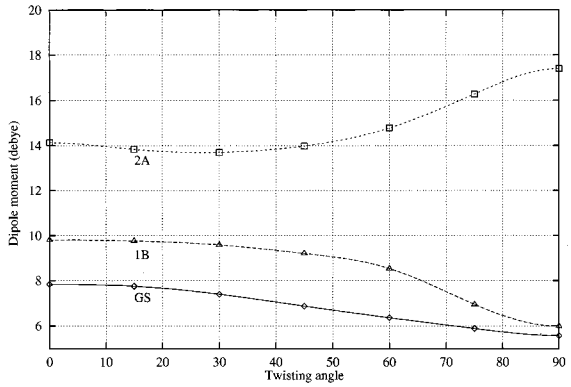

Figure 7. Ground and low-lying singlet excited states dipole moment curves of DMABN in vacuo as a function of the twisting angle. Dipole momens are in debye and angles in degrees.

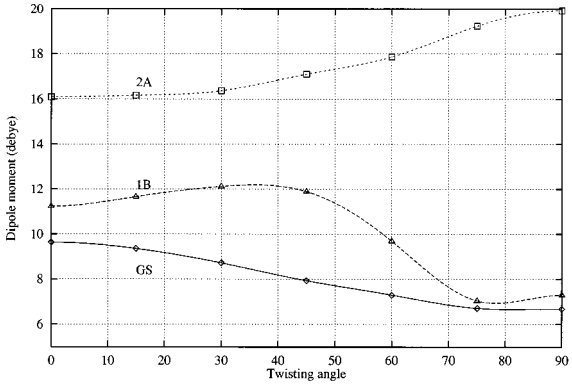

Figure 8. Ground and low-lying singlet excited state dipole moment curves of DMABN in acetonitrile as a function of the twisting angle. Dipole moments are in debye and angles in degrees.

In addition, the solvated system shows an unexpected maximum at around 40° which is not easy to explain; the small increment observed from 75° to 90° is likely due to numerical instabilities. The 2^1A state behaves differently. Its dipole moment is large already in the nontwisted conformation (around 14 D in vacuo and 16 D in acetonitrile) and it increases considerably with the twisting angle, showing a maximum at 90° in both cases. Once again the small shallow observed for this state in Figure 7 at around 30° has to be due to numerical instabilities. The comparison of the two curves shows that solvent interactions largely amplify the 2^1A dipole, thus allowing a stabilization of the state at each twisting angle.

Both the previous analyses (i.e., maps and twisting curves) are centered on general aspects of the phenomenon, but they have not really involved comparisons with experiments. In the following section we thus present the absorption and fluorescence energies obtained with CIPSI both in vacuo and in acetonitrile solution and the comparisons with experimental data; to complete the analysis of solvent effects we also present results obtained for an apolar solvent, namely, cyclohexane.

3.3. Absorption and Fluorescence Energies. Before presenting the numerical results, some preliminary comments will be reported. In the previous sections we introduced a problem which always appears when combining dynamical processes, such as electronic transitions, with the presence of a solvent. Details on this important phenomenon can be found in different papers;[30,31] here we only recall some basic aspects.

The electronic transitions involved in both absorption and fluorescence are generally characterized by very fast time scales. In a continuum solvation approach such as that exploited here, this means that the perturbation representing the response of the solvent molecules to the introduction of a solute (i.e., their polarization) feels a fast change in the polarizing field which it will or will not manage to follow. The time-coherence between changes in the solute and in the solvent will depend on the relaxation times characterizing the degrees of freedom of both the single molecules and the bulk of solvent. In the specific case of vertical electronic transitions, i.e., very rapid changes in the distribution of electronic charge not involving nuclear motions, it is sufficient to assume that the solvent presents two types of response, one related to its electrons and the other to all the rest (nuclear vibrations, rotations, etc.), and that the former is by far faster than the latter. In this approximation, usually indicated as Pekar partition, the solvent will modify its status (i.e., its polarization) during the solute electronic transition only as concerns the fast contribution; on the contrary, the other, and main, part of its response will remain frozen to the original situation before the change.

Table 1. Absorption Energies (eV) for Planar DMABN in Vacuo and in Solution[a]

	CIPSI		exp	
	1^1B	2^1A	LE	CT
vacuum	4.29	4.78	4.25[a]	4.56[a]
acn	4.00 (4.06)	4.10 (4.01)	n.o.	4.2[b]
cyc	4.00	4.32	4.1[b]	4.4[b]

[a] "acn" indicates acetonitrile as solvent while "cyc" refers to cyclohexane. Values in parentheses refer to equilibrium calculations (see text for details). Experimental data refer to absorption maxima.

In our framework, this partial response can be described in terms of an electrostatic interaction not determined by the full static dielectric constant but by its electronic contribution only, i.e., the optical dielectric constant $\epsilon_{opt} = n^2$, where n is the solvent refractive index. The difference between ϵ_{stat} and ϵ_{opt} strongly depends on the intrinsic characteristics of the solvent, namely, for polar solvents $\epsilon_{opt} < \epsilon_{stat}$, with very large differences in the case of high polarity, while for nonpolar solvents $\epsilon_{opt} \simeq \epsilon_{stat}$.

This model properly applies only to the electrostatic part of the solute−solvent interaction; the repulsion term, in fact, will follow completely independent rules, mainly dictated by the difference in the spatial extent of the charge distribution in each electronic state; further comments can be found in ref 16.

In Table 1 we report absorption energies computed for DMABN in vacuo and in the two solvents through the CIPSI algorithm. The adopted geometries are those optimized for the ground states in gas phase and in each solution. As a comparison we also report experimental data.

To properly analyze solvent effects, it is necessary to first check the quality of the QM calculation. It is important to say that absorption values reported in Table 1 (and the fluorescence energies we shall present below) have been obtained by exploiting a more accurate CIPSI scheme with respect to that used to get the previous maps and curves (see Figures 2−8). Calculations of the whole spectrum of possible conformations

(30) Ooshika, Y. *J. Phys. Soc. Jpn.* **1954**, *9*, 594. (b) Marcus, R. *J. Chem. Phys.* **1956**, *24*, 966. (c) McRae, E. G. *J. Phys. Chem.* **1957**, *61*, 562. (d) Basu, S. *Adv. Quantum. Chem.* **1964**, *1*, 145. (e) Levich, V. G. *Adv. Electrochem. Eng.* **1966**, *4*, 249;

(31) Kim, H. J.; Hynes, J. T. *J. Chem. Phys.* **1990**, *93*, 5194 and 5211. (b) Berezhkosvskii, A. M. *Chem. Phys.* **1992**, *164*, 331. (c) Basilevski, M. V.; Chudinov, G. E. *Chem. Phys.* **1990**, *144*, 155. (d) Aguilar, M. A.; Olivares del Valle, F. J.; Tomasi, J. *J. Chem. Phys.* **1993**, *98*, 7375. (e) Cammi, R.; Tomasi, J. *Int. J. Quantum Chem: Quantum Chem. Symp.* **1995**, *29*, 465. (f) Mikkelsen, K. V.; Cesar, A.; Ågren, H.; Jensen, H. J. Aa. *J. Chem. Phys.* **1995**, *103*, 9010. (g) Mennucci, B.; Cammi, R.; Tomasi, J. *J. Chem. Phys.* **1998**, *109*, 2798.

at the same level of accuracy would have in fact required a too heavy computational effort which at the end would have not added too much to the previous analysis.

For DMABN in vacuo, CIPSI excitation energies of 4.29 and 4.78 eV are computed for the first and second excited state. The first excitation energy is in very good agreement with the experimental data of 4.25 eV obtained in ref [32] while for the second one a discrepancy of 0.2 eV is found. Previous accurate calculations carried out at the CASPT2 level with a rather large basis set gave 4.05 and 4.41 eV, thus showing the difficulty in comparing computed vertical excitation energies with experimental data. As already discussed in the previous section, in vacuo the first excited state has B symmetry and is only a weakly allowed transition (the computed oscillatory strength is 0.082). The most intense transition is into the second excited state with A symmetry (in this case the oscillatory strength is 0.786).

From experiments, it is well-known that the most intense absorption band corresponding to the excitation into the 2^1A state is red-shifted in the presence of polar solvents. The charge transfer character of this state, associated with a large dipole moment, in fact allows a by far more effective solvent-induced stabilization with respect to the less polar ground state. This effect is correctly reproduced by the results reported in Table 1. Both in acetonitrile and cyclohexane the excitation energies toward A are smaller than in vacuo and they decrease by increasing the polarity of the solvent. The agreement with the experimental evidence is not limited to a qualitative aspect, but for both transitions and both solvents a very good correspondence with observed results is found; for transition to 1^1B (or LE) in acetonitrile no experimental data are available due to the complete overlap of the bands.

We also note that the results of acetonitrile only apparently contradict what is reported in the previous section. The analysis of twisting curves showed that the A state is so effectively stabilized in acetonitrile that it becomes the lowest excited state, thus inverting the situation found in the gas phase. In Table 1, on the contrary, the excitation energy toward B (4.00 eV) is smaller than that toward A (4.10 eV), indicating a shift in the order of the excited states with respect to what is reported in Figure 6.

This apparent contradiction can be explained by resorting to the nonequilibrium scheme discussed at the beginning of the section. In the calculation of absorption energies, in fact, we assume that the slow component of the solvent response cannot immediately follow the fast change and thus it remains fixed as in the ground state. This means that in the excited state the solute sees a solvent only partially modified with respect to the initial situation, and thus it cannot be stabilized as efficiently as in the case of a complete response (i.e., assuming a full solute−solvent equilibrium). If we consider that for acetonitrile the static dielectric constant is 36.64 while the optical analogue is only 1.806, it is easy to see the discrepancies between equilibrium and nonequilibrium results. To have a more direct comparison with the parallel equilibrium scheme exploited to compute twisting curves in Table 1, we report also the equilibrium excitation energies. This scheme cannot be applied to cyclohexane for which $\epsilon_{opt} \simeq \epsilon_{stat}$, and thus there are no appreciable changes when nonequilibrium effects are introduced.

The analysis above on the possible interactions leading to the observed solvent effects on the absorption spectra is supported by values of dipole moments for each state in vacuo and in solution. In Table 2 we report the dipole moments of ground and excited states of planar DMABN both in vacuo and in the two solvents with indication of the experimental data, when available.

Table 2. Dipole (debye) of Ground and Excited States of Planar DMABN in Vacuo and in Two Solutions[a]

	CIPSI			exp	
	GS	1^1B	2^1A	GS	LE
vacuum	7.73	9.79	13.61	5−7[b]	8−11[b]
acn	9.82	12.13	15.34		
cyc	8.59	10.82	14.23		∼10[c]

[a] "acn" indicates acetonitrile as solvent while "cyc" refers to cyclohexane. Ranges of data reported for gas-phase collect many available experimental values obtained in various apolar solvents. [b] Reference 9 and references therein. [c] Reference 34.

Upon excitation the dipole moments of all the states increase, as predicted by considering the previous analysis on the nature of the orbitals involved in the two excitations. In fact, the π^* orbital, which characterizes both the excited states, is more localized toward the cyano group than the π orbital (i.e., the initial orbital as concerns excitation to B) and than the mixed $\pi-$n orbital (involved in the transition to A). Such an increase in the dipole is amplified in the presence of a polar solvent which stabilizes most the states with larger dipolar character.

For the emission spectra, the experimental finding is that two distinct bands are found in acetonitrile (centered at 3.4 and 2.6 eV, respectively),[33] thus leading to the phenomenon of dual fluorescence, and that in the nonpolar cyclohexane a very weak CT band at 3.2 eV is found in addition to the strong normal LE fluorescence at 3.6 eV; no clear data are available for the gas phase.

The geometries used for the excited states are those obtained with CIS optimizations both in vacuo and in solution; only in cyclohexane we have not been able to find a real minimum at a 0° or at a 90° twisting angle. Thus, in this case, geometries are those of the ground state, with the amino group rotated 90° in the twisted structure. For a comment on the quality of CIS geometry and for a detailed analysis of the geometries of each state, we refer readers to the original paper on the CIS-IEF method;[16] here we only recall that the main aspect to observe for all the excited structures when compared to the corresponding ground-state geometry is the strong increase in the phenyl bond lengths at the substituent-bearing carbons. On the contrary, the bond lengths of the carbons between (here represented by $R_{C_2C_3}$) become shorter. In both the twisted structures a significant decrease with respect to the corresponding ground-state value of the amino-ring bond is observed; this can be tentatively explained in terms of the charge transfer from the donor to acceptor part of the molecule which leads to a positively charged amino group. We also recall that CIS optimization for the 2^1A state in vacuo has led to a twisting angle of 90° while the CIPSI curve reported in Figure 5 shows a minimum around 75°. This discrepancy can be imputed to two different reasons. On the one hand, in the CIS optimization all geometrical parameters have been relaxed while in the CIPSI curve the geometry is kept frozen to the GS structure, and on the other hand the QM levels adopted in two calculations are different. In any case, the flat shape of the 2A twisting curve in Figure 5 for large angles (70−90°) ensures that the results cannot significantly change for a slight shifting of the angle which characterizes the CT minimum. In addition, we recall that also previous CASPT2[7] and DFT/CIS[9] calculations find a flat potential curve

(32) Bulliard, C.; Allan, M.; Wirtz, G.; Haselbach, E.; Zachariasse, K.A.; Detzer, N.; Grimme, S. *J. Phys. Chem. A* **1999**, *103*, 7766.

(33) Lipinski, J.; Chojnacki, H.; Grabowski, Z.R.; Rotkiewicz, K. *Chem. Phys. Lett.* **1980**, *70*, 449.

Table 3. Fluorescence Energies (eV) at Planar and Twisted Conformations for DMABN in Vacuo and in Two Solvents[a]

	CIPSI		exp	
	planar	twisted	LE	CT
vac	4.24	3.53		
acn	3.87	2.50	(3.4)[b]	2.6[b]
cyc	4.00	3.44	3.6[b]	(3.2)[c]

[a] "acn" indicates acetonitrile and "cyc" cyclohexane. The parentheses indicate that the value is very uncertain as the band is apparent as a broadening of the emissium spectrum without a distinct maximum. Experimental data refer to fluorescence maxima. [b] Reference 33 and references therein. [c] Reference 34.

for the 2^1A state with a shallow minimum at intermediate twisting angles, thus showing a difficult univocal identification of the exact minimum.

The results of our calculations for 0° and 90° twisted DMABN both in vacuo and in solvents along with experimental results are summarized in Table 3.

With respect to the gas-phase data, for which no experimental confirmation can be achieved, it is more interesting to analyze results obtained in acetonitrile. The results reported in Table 3 show a very good agreement for the second, or anomalous, fluorescence (the discrepancy is 0.1 eV), while the behavior found for the first, or normal, fluorescence is not as good. However, we have to recall that in polar solvents the CT (2^1A) band dominates and the LE (1^1B) band is observed as a shoulder on the very broad CT band. Furthermore, the lifetime of the LE state is very short, in the picosecond region (it is in fact a largely permitted state), while the lifetime of the A state is in the nanosecond region.[34] All these aspects should lead to a large uncertainty in the experimental data for 1^1B.

In cyclohexane, for which we have not reoptimized the geometries of the excited states but used that obtained for the GS (rotating the amino group of 90° in the twisted structure), both fluorescence energies are too high with respect to the experiments. This findings could be explained in terms of the missing geometry contribution; in fact, a transition from a relaxed geometry, corresponding to a minimum for the excited state of interest, is always lower than that from a nonequilibrium geometry and thus, considering geometry changes, should lead to a better agreement with the experiments.

As previously stated, no comparisons with experiments can be made for the gas-phase results; however the values, if it were possible, should be expected to be at higher energy with respect to cyclohexane, and thus our calculations are in the right direction.

Conclusions

In the present work we have studied DMABN with a perturbed multirefence CI method including solvation effects via the PCM-IEF model. For the first time solvent effects are taken into account both in the geometries and in the properties of ground and excited states.

To verify the reliability of the various models proposed so far to study this system, we have initially run calculations for the isolated system in different geometrical conformations. The results have allowed us to build wagging−twisting energy maps, confirming the main role of the twisting coordinate as predicted by the TICT model. This analysis on the most plausible charge-transfer mechanism has been further extended to the solvated system; in particular, we have computed energies and dipole moments for the two lowest excited states in acetonitrile solution along the wagging coordinate. These analyses have shown that the wagging motion, without twisting, is unable to provide the highly polar state responsible for the CT fluorescence in polar solvents. Supported by these findings, we have limited the main body of the analysis to the twisting motion only and thus recomputed energy curves with respect to the twisting angle in the presence of solvent effects. Such an analysis has been then completed with calculations of absorption and fluorescence energies in vacuo and in both polar and apolar solvents.

The results we have obtained have allowed us to rationalize better the lack of CT fluorescence in the gas phase and its appearance in polar solvents, supporting the TICT model of Grabowski et al. when differently applied to isolated and solvated systems.

Previous calculations already managed to describe, and in some cases with great accuracy, the mechanism usually suggested for normal fluorescence in the gas phase, i.e., first a deactivation to the S_1 state from the S_2 state initially reached through the vertical absorption and then the emission from the S_1 state still at zero twisting angle (at this geometry S_1 corresponds to the so-called LE state). On the contrary, no numerical evidence has been given for the second, or "anomalous" fluorescence, which would occur only after an intramolecular twisting motion along the S_1 surface leading from the original LE state to the final CT state. In fact, in vacuo calculations can only show that such a reaction does not occur due to the energy barrier in the S_1 hypersurface (and this is the evidence shown in both Figure 3 and Figure 5). However, by explicitly including solvent effects one can see that such a barrier is lower in polar solvents in which the S_1 state is represented by a CT state already at a 0° twisting angle (as shown in Figure 6).

We recall that the results obtained for absorption and fluorecence energies involve a nonequilibrium condition between solute and solvent. It is well-known that, in polar solvents, the relative stabilization of excited states of molecular solutes depend on the response times of the solvent molecules; however, reliable numerical proofs of this phenomenon are rare to find. The results we have obtained for DMABN in acetonitrile can give useful hints on this aspect. In fact, at the planar geometry, the two lowest singlet excited states which are very close in energy but very different with respect to the dipolar character are differently ordered depending on if a fully or a partially equilibrated solvent is considered. This finding, of interest also for further studies on the optical properties of this and similar systems, shows the sensibility of the PCM-IEF solvation model and its potentialities as a computational tool to explain excitation processes in solution.

The theoretical and computational approach proposed in the present paper can be improved, mostly with respect to the interactions included in the solvent operator; here, for example, dispersion effects between solute and solvent molecules are completely neglected. However, this study represents one of the first attempts to treat solvent modifications in both geometry and charge distribution of ground and excited electronic states of a relatively complex molecule. Previous attempts in this direction, in fact, have been limited to small molecules or to inaccurate QM calculations. On the contrary, the linking of a good QM level for the solute and an accurate model for the solvent, which is also strongly coupled to the description of the solute wave function, seems to be the best approach to study photophysical phenomena involving different electronic states.

(34) Reference 5a.

JA000814F